NMR on Oriented ^{131}I Nuclei Implanted in Single-Crystal Iron: Observation of Vacancy-Associated Impurity Sites

D. Visser, L. Niesen, H. Postma, and H. de Waard
Laboratorium voor Algemene Natuurkunde, Groningen, The Netherlands
(Received 16 June 1978)

Nuclear magnetic resonance was performed on oriented ^{131}I nuclei implated in single-crystal iron. Apart from the substitutional resonance, satellite resonances were found whose number and position depended on the angle between the magnetic field and the crystal axes. These lines are found to originate from impurity sites that have a neighbor vacancy, creating an electric field gradient of 1.05×10^{22} V/m^2 along one of the ⟨111⟩ axes.

Hyperfine-interaction (hfi) measurements on implanted radioactive nuclei in metals probe the immediate environment of the implanted impurities and thus are well suited to study implantation-induced damage. In this Letter we show that besides Mössbauer spectroscopy (MS) and perturbed angular correlations (PAC) used before for this purpose,[1] the technique of nuclear magnetic resonance on oriented nuclei (NMR/ON) has unique capabilities: The precise nature of specific damage sites can be unambiguously derived on grounds of symmetry alone.

We implanted ^{131}I ions into several single crystals of iron, with different orientations of the crystal axes relative to the crystal edges. From previous MS studies on the system[2] I*Fe* it was found that roughly 40% of the implanted I ions end up substitutionally, in regular lattice sites. These show the largest hfi. Another 30% is found in sites with about 20% smaller hyperfine field (intermediate-field sites). The last 30% land in sites with much reduced field (low-field sites). The simplest explanation for the intermediate-field sites would be that atoms in these sites have one vacancy in the nearest-neighbor shell. Channeling measurements of Callaghan, James, and Stone[3] give extra evidence for the existence of such sites. ^{129}I Mössbauer spectra obtained with ^{129m}Te*Fe* sources have been explained in the same way.[4] In this case the intermediate field is roughly 90% of the substitutional field.

NMR/ON experiments on ^{131}I*Fe* sources were first performed by James, Stone, and Forster[5] and Stone.[6] A narrow resonance line was found at 684 MHz because of ^{131}I in substitutional sites, but there was no evidence for intermediate-field sites. Schoeters *et al.*[7] reported the observation of a shallow and broad intermediate-field resonance in the neighboring system ^{129m}Xe*Fe*, using polycrystalline iron.

In order to obtain detailed information on the nature of the intermediate-field site we used different orientations of the crystal with respect to the direction of the external magnetic field. Three crystals were cut from single-crystal plates of 0.9 mm thickness and 99.98% purity, with their longest dimension along a ⟨100⟩, ⟨110⟩, and ⟨111⟩ axis.

Implantations were done with the Groningen isotope separator at an energy of 110 keV. The implanted doses were 3.5×10^{13}, 2.2×10^{14}, and 3.2×10^{13} atoms/cm^2, respectively. Source strengths were about 200 μCi. An external field was applied horizontally along the longest dimension of the crystal. All crystals showed saturation of the anisotropy $W(0)-1$ at external fields exceeding the demagnetizing fields by 0.03–0.06 T. The saturation value, $W(0)\simeq1.17$ at a temperature of 25 mK, is in agreement with earlier measurements[8] and shows that roughly 30% of the ^{131}I nuclei cannot be oriented at this temperature.

Each NMR run was performed with a sequence of 128 steps up and 128 steps down in frequency across the expected resonance frequencies. Frequency modulation (FM) was applied during each odd sequence. $W(0)$ of the 364-keV transition was monitored with two 3-in.×3-in. NaI(Tl) detectors, the counts of which were added and stored into the memory of a 512-channel analyzer, synchronized to the rf oscillator. The rf-power level was chosen such that at most 30% of the initial anisotropy was lost because of eddy-current heating. Because of the imperfect match of rf coil and transmission line, the rf power was not constant over the whole frequency range. The resulting variations in $W(0)$ were (1–2)%.

The differences in counting rate with FM off and on, translated to changes in anisotropy, are plotted as a function of frequency for three of the runs in Fig. 1. The run for the crystal with $B_{\rm ext}(\|\langle110\rangle)=0.150$ T shows, apart from the substitutional resonance line, two satellite lines at 623.1(3) and 643.0(4) MHz. The percentage of the anisotropy destroyed in each line, given by

$A/\Delta\nu_{FM}$ (A is the area under the peak and $\Delta\nu_{FM}$ is the peak-to-peak amplitude of the FM; 2 MHz in this case), turned out to be 3.8% and 3.0%, respectively, whereas 15% of the anisotropy was destroyed at the substitutional resonance during this run. The run for the crystal with $B_{ext}(\parallel\langle 100\rangle) = 0.125$ T shows only one satellite at 633.5(2) MHz; i.e., at the center of gravity of the doublet, 3.9% of the anisotropy was destroyed in this line. The run for the crystal with $B_{ext}(\parallel\langle 111\rangle) = 0.125$ T shows lines at 625.9(2) MHz (anisotropy destruction 3.1%), 6.39.0(3) MHz (destruction 2.1%), and 654.6(2) MHz (destruction 2.4%).

Figure 2 gives examples of substitutional resonances in the three crystals. The true substitutional resonance is superimposed on a broader resonance, probably originating from radiation damage at some distance of the impurity. This phenomenon was reported earlier by Stone.[6] The substitutional resonance frequencies extrapolated to zero internal field were 683.80(10) MHz for $\vec{B}\parallel\langle 100\rangle$, 684.04(5) MHz for $\vec{B}\parallel\langle 110\rangle$, and 683.88(5) MHz for $\vec{B}\parallel\langle 111\rangle$, whereas the smallest widths obtained were ~ 1 MHz for all crystals. The maximum destruction of anisotropy obtained, including the broad resonance structure, was (50–60)% in each case, yielding a substitutional fraction of about 35%.

In the presence of a local distortion of the cubic environment, the hyperfine-interaction Hamiltonian at the ^{131}I nucleus can be written as

$$H_{hfi} = -g_N\mu_N(B_{hf}+B_{ext}-\mu_0 NM)I_z - g_N\mu_N\vec{B}_{dip}\cdot\vec{I} + \frac{e^2qQ}{4I(2I-1)}[3I_{z'}^2 - I(I+1)+\eta(I_{x'}^2 - I_{y'}^2)], \quad (1)$$

where the z axis points along the external field $\vec{B}_{ext}$ and the z' axis defines the direction of the distortion. The shape-dependent demagnetizing field $\mu_0 N\vec{M}$ is 0.086 T for the $\langle 110\rangle$ crystal, 0.066 T for the $\langle 100\rangle$, and 0.053 T for the $\langle 111\rangle$ crystal (N is the demagnetizing factor and $\vec{M}$ the magnetization). We assume that the hyperfine field $\vec{B}_{hf}$ is purely of the contact type and neglect any anisotropic magnetic hfi, which seems reasonable for a diamagnetic atom like I in a metallic environment. As usual, the Lorentz field $\frac{1}{3}\mu_0\vec{M}$ is included in $\vec{B}_{hf}$.

The experimental results can be explained very well by assuming that the ^{131}I atoms producing the satellite resonances have a vacancy on a nearest-neighbor position, which creates an electric field gradient (EFG) eq along one of the $\langle 111\rangle$ directions. Even if we take into account that the vacancy will cause the lattice to relax,[9] this $\langle 111\rangle$ direction remains an axis of threefold symmetry, creating an axial symmetric EFG ($\eta = 0$).

At the same time, the vacancy will give a dipo-

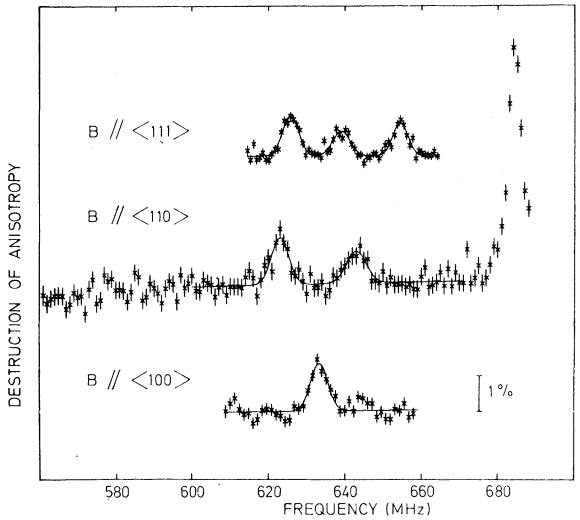

FIG. 1. NMR/ON resonances for three different orientations of the applied field with respect to the crystal axes.

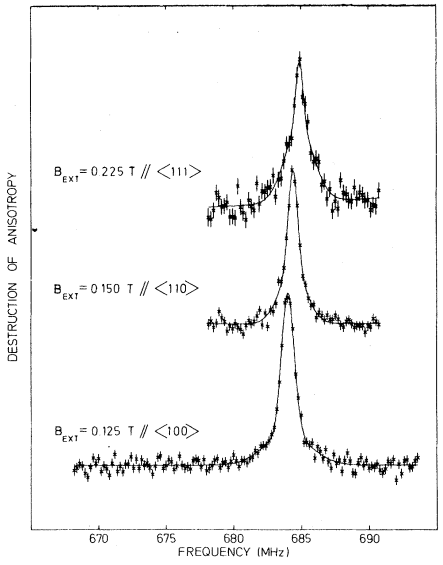

FIG. 2. NMR/ON resonances for substitutional ^{131}I in iron, for three different directions of the applied field. Drawn curves are two-component fits, as explained in the text.

lar-field contribution $\vec{B}_{dip}$ exactly opposite to that of a single Fe moment μ at the same distance r. For the z component of this field we have $B_{z,dip} = -(\mu_0\mu/2\pi r^3)P_2(\cos\theta)$, where θ is the angle between the z and the z' axis. Using $\mu = 2.2\mu_B$ and $r = 2.48$ Å, we obtain $B_{dip} \equiv \mu_0\mu/2\pi r^3 = 0.267$ T. Lattice relaxation and the partial nonlocalization of the Fe moment will affect the magnitude of $\vec{B}_{dip}$, but not the $P_2(\cos\theta)$ dependence.

Neglecting off-diagonal elements of the hfi Hamiltonian we obtain for the hfi energy levels

$$E_m = -g_N\mu_N[B_{hf} + B_{ext} - \mu_0 NM - B_{dip}P_2(\cos\theta)]m + \frac{e^2qQ}{4I(2I-1)}P_2(\cos\theta)[3m^2 - I(I+1)]. \quad (2)$$

For each angle θ, the resonance will be split into $2I$ (=7) components separated in frequency by $\Delta\nu_Q = e^2qQP_2(\cos\theta)/14h$. We have calculated the relative changes in anisotropy (assuming complete saturation) for each of the possible $\Delta m = \pm 1$ transitions at the temperature of the measurement, $T \simeq 37$ mK. It is found that the effect of the transition between the lowest two levels is a factor of 10 larger than that of the other transitions.

For $\vec{B} \parallel \langle 100\rangle$ we expect to see only the magnetic hfi, because $P_2(\cos\theta) = 0$ for all $\langle 100\rangle$–$\langle 111\rangle$ angles. For $\vec{B} \parallel \langle 110\rangle$ the possible geometries give $P_2(\cos\theta) = \pm\frac{1}{2}$, so that two quadrupole split patterns should be found, centered around the line observed with $\vec{B} \parallel \langle 100\rangle$. The signal-to-noise ratio in our experiments only permits us to see the transitions between the lowest two levels, with separation depending on eq and B_{dip}.

The measurement with B_{ext} ($\parallel\langle 111\rangle$) = 0.125 T can be used to obtain the sign of e^2qQ. In this case $P_2(\cos\theta) = 1$ for two nearest neighbors whereas $P_2(\cos\theta) = -\frac{1}{3}$ for the other six. The resonance lines observed at 625.9 and 654.6 MHz are in agreement with the expected pattern and yield $e^2qQ < 0$. However, we observe a strong deviation from the theoretical intensity ratio 3:1 for these lines and find an additional resonance at 639.0 MHz. Both phenomena are not understood at the moment.

We conclude that the satellite resonances are caused by impurities with one nearest-neighbor vacancy (S_{2v} sites), creating an EFG along one of the $\langle 111\rangle$ axes. This conclusion is unique: We can rule out other small impurity vacancy clusters because these would have different EFG axes. This is true in particular for an association of the ^{131}I impurity with two vacancies. In that case, the I atom would relax to the center of a trivacancy[9] and experience a nonaxial EFG with completely different principal axes.

With $B_{dip} = 0.26$ T, a fit to our experimental resonance frequencies using Eq. (1) gives $\nu_B = g_N\mu_N B_{hf}(S_{2v}) = 632.8(3)$ MHz and $e^2qQ/h = -104(5)$ MHz. With the known nuclear moments of ^{131}I [$\mu/\mu_N = 2.738(1)$, $Q = -0.41(1)$ b [10] we obtain $B_{hf}(S_{2v}) = 106.1(5)$ T and $eq = 1.05(5)\times 10^{22}$ V/m^2. Neglecting B_{dip} would lower eq by 8%.

The lattice contribution to the EFG due to one vacancy is calculated to be[7] $eq = -4.5\times 10^{20}$ V/m^2. This contribution will be enhanced at the impurity nucleus by the Sternheimer antishielding factor and by the effect of the conduction electrons. In this particular case, both effects are difficult to evaluate without a detailed knowledge of the electronic structure of the impurity, but our enhancement factor of about 20 is a reasonable value. The sign of eq indicates that the conduction electrons overcompensate the lattice contribution to this vacancy-induced EFG, as is generally observed in noncubic metals.

Although we used as much rf power as possible, we probably could not saturate the satellite resonances, as shown by the fact that we could destroy only 15% of the anisotropy in the substitutional resonance for the run displayed in Fig. 1. Therefore, we cannot draw any conclusions about site occupations from the measured peak areas. Finally, we note that in polycrystalline iron the satellite resonance would be smeared out over a region of ~ 30 MHz and consequently it would be too shallow to be observed. Clearly, the use of single crystals is essential for successful NMR/ON experiments on damage-associated sites created by ion implantation.

The authors wish to thank Dr. P. M. Bronsveld for his help in preparing and analyzing the Fe single crystals and Mr. J. J. Smit for performing the ion implantations. This work is financially supported by the Stichting voor Fundamenteel Onderzoek der Materie (FOM), subsidized by the Nederlandse Organisatie voor Zuiver Wetenschappelijk Onderzoek (ZWO).

[1] G. Vogl, Hyperfine Interact. 2, 151 (1976), and references therein.

[2]H. de Waard, R. L. Cohen, S. R. Reintsema, and S. A. Drentje, Phys. Rev. B 10, 3760 (1974).
[3]P. T. Callaghan, P. K. James, and N. J. Stone, Phys. Rev. B 12, 3553 (1975).
[4]S. R. Reintsema, H. de Waard, and S. A. Drentje, Hyperfine Interact. 2, 367 (1976).
[5]P. K. James, N. J. Stone, and H. R. Forster, in *Proceedings of the International Conference on Hyperfine Interactions Studied in Nuclear Reactions and Decay, Uppsala, Sweden, 1974*, edited by E. Karlsson and R. Wäppling (University of Uppsala, Uppsala, Sweden, 1974), p. 156.
[6]N. J. Stone, Hyperfine Interact. 2, 45 (1976).
[7]E. Schoeters, R. Coussement, R. Geerts, J. Odeurs, H. Pattyn, R. E. Silverans, and L. Vanneste, Phys. Rev. Lett. 37, 302 (1976).
[8]B. K. S. Koene and H. Postma, Nucl. Phys. A219, 563 (1974).
[9]S. A. Drentje and J. Ekster, J. Appl. Phys. 45, 3242 (1974).
[10]E. Lipworth, H. L. Garvin, and T. Green, Phys. Rev. 119, 2022 (1960).

Model for the Temperature Dependence of the Metastable 2 × 1 Reconstructed Silicon (111) Surface

C. T. White and K. L. Ngai
Naval Research Laboratory, Washington, D. C. 20375
(Received 24 April 1978)

We develop a model based on the idea of dangling-bond–mediated attractive electron-electron interactions to describe the metastably reconstructed 2×1 Si(111) surface and its elimination with increasing annealing temperature. It is found that the resultant picture is able to correlate a considerable amount of experimental data.

Low-energy electron-diffraction (LEED) studies of vacuum-cleaved Si(111) surfaces have yielded a crystallographic surface structure appropriate for a 2×1 unit mesh.[1] It is generally agreed[1-5] that this LEED pattern arises essentially from the displacement (reconstruction) of alternate rows of surface atoms inward and outward from where they would sit if the bulk were ideally truncated. With increasing annealing temperature[1,5] the 2×1 structure is transformed to an effective 1×1 structure in the vicinity of 600°K, which is then followed within ~60°K by a 7×7 structure. The 2×1 is apparently not thermodynamically recoverable and hence metastable. A considerable number of experiments have been performed which show a well-defined correlation between the LEED-observed (2×1)-(1×1) transition and changes in the electronic structure of the system.[1,5-9] However, so far no theoretical picture has been developed which can satisfactorily interpret these observations. In fact little if any theoretical attention has been given to the effects of temperature on the 2×1 reconstructed surface.

Since the cleavage-prepared 2×1 is metastable, it must be separated by a free-energy barrier from the more stable structures of the system. It has been known for some time that there is a correlation between enhanced stability of the 2×1 pattern and increasing cleavage-step density[1] and this fact could lead one to identify these steps ultimately with the origin of the 2×1. However, most recent experimental studies[10] indicate that the 2×1 pattern does not arise because of the steps but is rather an intrinsic metastable structure of the Si(111) surface and only somewhat further stabilized by the steps. In this note we propose a model of the Si(111) surface which attributes the existence of the metastable 2×1 to a correlated self-trapping of the surface dangling-bond electrons (and holes). As will be seen the resultant picture provides new insight into the interplay between the crystallographic and electronic features of the surface.

Our model is described by the Hamiltonian

$$H=\sum_{i\sigma}E_h n_{i\sigma}-\sum_i(\lambda_1 u_i+\tfrac{1}{2}\lambda_2 u_i^2)(n_{i\uparrow}+n_{i\downarrow}-1)$$
$$+\sum_{ij\sigma}V_{ij}a_{i\sigma}^{\dagger}a_{j\sigma}+\tfrac{1}{2}C\sum_i u_i^2+\sum_i U n_{i\uparrow}n_{i\downarrow}, \quad (1)$$

where the sites $\{i\}$ form a triangular lattice; σ takes on two values up ($\uparrow$) or down ($\downarrow$); $a_{i\sigma}^{\dagger}$ and $a_{i\sigma}$ are creation and annihilation operators, respectively, for electrons of spin σ in the surface dangling hybrid $|i\sigma\rangle$; and $n_{i\sigma}=a_{i\sigma}^{\dagger}a_{i\sigma}$ is the usual occupation-number operator. Each quantity u_i is dimensionless and represents a normal displacement from the unreconstructed surface of a surface atom at the site i divided by the bulk bond length. This displacement can be either outward ($u_i>0$) or inward ($u_i<0$). The second term on the

